

# Enabling Fast Brain-Computer Interaction by Single-Trial Extraction of Visual Evoked Potentials

Min Chen · Jinan Guan · Haihua Liu

Received: 27 November 2010 / Accepted: 29 March 2011 / Published online: 18 June 2011  
© Springer Science+Business Media, LLC 2011

**Abstract** This paper investigates the challenging issue of enabling fast brain-computer interaction to construct a mental speller. Exploiting visual evoked potentials as communication carriers, an online paradigm called “imitating-human-natural-reading” is realized. In this online paradigm, single-trial estimation with the intrinsically real-time feature should be used instead of grand average that is traditionally used in the cognitive or clinical experiments. By the use of several montages of component features from four channels with parameter optimization, we explored the support vector machines-based single-trial estimation of evoked potentials. The results on a human-subject show the advantages of the inducing paradigm used in our mental speller with a high classification rate.

**Keywords** Body area networks · Brain-computer interface (BCI) · Evoked potentials · Feature selection · Single-trial estimation · Support vector machine (SVM)

## Introduction

Advances in wireless communication technologies, along with the availability of wearable and low-cost bio-sensors

---

M. Chen  
School of Computer Science and Engineering,  
Seoul National University,  
Seoul, Korea  
e-mail: minchen@ieee.org

J. Guan (✉) · H. Liu  
School of Electronic Engineering,  
South-Central University for Nationalities,  
Wuhan 430074, China  
e-mail: guanja@mail.scuec.edu.cn

H. Liu  
e-mail: lhh@mail.scuec.edu.cn

open the possibility to realize human’s expectation flexibly through a body language user interface. For example, Digital-Being exploits body area networks [1] to enable dancers to express their feelings and moods by dynamically and automatically adjusting music and lighting in a dance environment to reflect the dancers’ arousal states while presenting their gestures and body movements [2].

If BAN technology can be incorporated with Brain-Computer Interfaces (BCI) technology, the information from the human neural system can directly tell other systems to have the correct and desired actions with the occurrence of different events to an object. The operation of BCI depends on the users’ intentions, which are encoded in electroencephalogram (EEG) signals; and then the system detects these features and converts them into control signals for export. At present, scalp electrodes are widely used for recording EEG signals generated by brain activities, so as to realize the communication with the outside, this is a non-destructive technology. However, the signals become very fuzzy after attenuation and aliasing through skull and skin, and the signals are often contaminated by Electrooculography (EOG), myoelectricity, and external electromagnetic fields. Thus, it is very difficult to extract characteristic signals. Furthermore, the effective multi-job superimposed averaging method in traditional neurophysiological experiments is useless when confronted with the BCI environment, which requires real-time interaction.

In recent years, as studies of BCI gradually develop, in order to overcome the bottleneck of brain signal interpretations, and improve man-machine communication speed, the single-trial estimation of characteristic signals has become an objective of intense interest [3, 4], and some scholars have conducted fruitful works [5, 6]. Researchers have proposed the single-trial estimation of multiple features according to the features of communication carrier

signals of different brain-computer interface systems, such as public spatial subspace decomposition and the Fisher discriminate, isolated component analysis and subspace projections, Support Vector Machine (SVM), etc [4–7]. These methods have obtained good effects in BCI applications. However, most of them use the data of eight even tens of channels to form the characteristic quantity of a sorting algorithm; thus, signal processing was complicated and the increased number of channels restricted the promotion of BCI, which was a disadvantageous for practical applications.

In order to further increase communication speed and solve the visual fatigue caused by stimulus signal flickering [8, 9, 10], this paper exploits a paradigm called “imitating natural reading” to generate evoked potential to construct a brain-controlled spelling device based on existing works [11]. Due to the effective inhibitions of exogenous reactions, the signal-to-noise ratio of evoked potential component in EEG signal was enhanced greatly, which helps to improve the recognition accuracy of characteristic signal. SVM is a machine learning method based on kernel functions, which is better than traditional artificial neural networks and has been extensively used in various pattern classifications for its solid mathematical foundation and good generalization ability. As the experiment for researching signal separability, this paper uses the  $\nu$ -SVM algorithm and different feature combinations of channels for pattern classifications of both target and non-target stimulus signals. The results on a human-subject show a perfect classification rate of 98.9%, and verify the advantages of the inducing paradigm used in our mental speller.

The rest of the paper is organized as follows. Section [Related works](#) presents related work. We describe the architecture and design issues of the proposed system in Section [System architecture](#) and Section [System implementation](#). In Section [Experimental results](#) presents the experiment results. Finally, we concludes our paper in Section [Conclusions](#).

## Related works

This paper is closely related to brain-computer interface and support vector machine classifier. In the following discussion, we briefly review the existing works and background knowledge.

### Brain-computer interface

To communicate with the external world, and even to control ambient environments using the conceptual work signals of brain is the dream of all humans of all ages.

The brain-computer interface (BCI) technology is a scientific method to realize this dream. It is a brain-computer (computer or other devices) communication system independent of normal output channels of the brain (i.e. peripheral nerve and muscle) [10]. The input of BCI is typically based on electroencephalogram (EEG) signals, which can be collected by an EEG sensor. The EEG sensor measures the electrical activity within the brain by attaching small electrodes to the human’s scalp at multiple locations. Then, information of the brain’s electrical activities sensed by the electrodes is forwarded to an amplifier for producing a pattern of tracings. Synchronous electrical activities in different brain regions are generally assumed to imply functional relationships between these regions. In a hospital, the patient may be asked to breathe deeply or to look at a flashing light during the recording of EEG [12].

The latest technology and computer innovation might allow a system to not only detect body language [13] but also respond to it. Through the integration of BCI with other technologies, such as BAN [14, 15], video surveillance and sensor networks, etc., wearable and wireless human-machine interface can be implemented [16]. Then, more and more automatic applications can come true in future.

### Support vector machine classifier

This section focuses on some background about SVM method, which is based on the statistical learning theory, and seeks the best compromise between complexity (i.e. learning accuracy of special training samples) and learning ability (i.e. ability to identify arbitrary samples faultlessly) of the models, according to limited sampling information, so as to obtain the best generalized ability. Its basic idea is as follows, non-linear separable patterns of the input space was converted into linear separable patterns in high dimensional feature space through non-linear function images, and then, the optimal classification face was determined in the linear separable state; the basic idea of which was described by Fig. 1 [17]. The solid and hollow points in the figure represent two classes of sample sets, namely,  $(x_i, y_i)$ ,  $i = 1, \dots, n$ ,  $\mathbf{x} \in R^N$ ,  $y \in \{+1, -1\}$ .  $H$  denotes the classification face, while  $H_1$  and  $H_2$  represent the samples closest to the classification face and the plane parallel to the classification face, respectively, in each class; and their distance  $\gamma$  is called the class interval. The optimal classification face meant that the classification face can correctly separate two classes (training error ratio was 0), as well as maximize the class interval. Here, the class interval  $\gamma$  equals to  $2/\|\mathbf{w}\|$  in order to maximize the interval to the equivalent of a minimized  $\|\mathbf{w}\|^2$ . The existence of wrongly classified samples can be allowed by leading in the positive

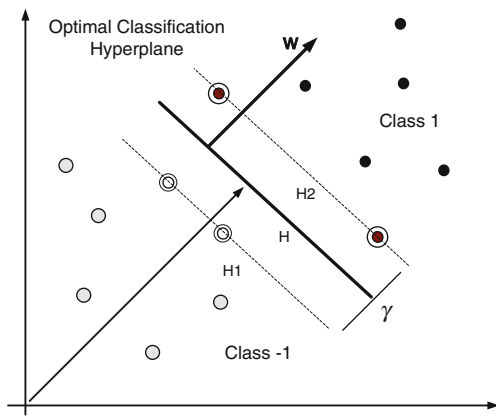


**Fig. 1** SVM looks for the optimal classification hyperplane (heavy line H) by maximizing class interval  $\gamma$ , and the two classes are separated in the feature space. Hyperplane H is determined by W and b, the calculation of W and b is completed by a support vector (dotted lines H1 and H2 and points with circle)

relaxation factor  $\xi_i$  to form a punishment term, so that the optimization problem with a so-called soft interval was derived.

$$\min \frac{1}{2} \|w\|^2 + C \sum_i \xi_i \tag{1}$$

$$\text{Subject to } y_i[(w \cdot x_i) + b] \geq 1 - \xi_i \tag{2a}$$

$$\text{And } \xi_i > 0 \tag{2b}$$

The classification face meeting the above conditions was the optimal classification face, where the training sample points in H1 and H2 were called support vectors. The aforesaid optimal classification face problem can be converted into a dual problem by using the Lagrange optimization method, i.e. under constraint conditions:

$$\sum_{i=1}^n y_i \alpha_i = 0, \tag{3a}$$

$$\text{and } 0 \leq \alpha_i \leq C \tag{3b}$$

for  $\alpha_i$  figuring out the maximum value of the function

$$Q(\alpha) = \sum_{i=1}^n \alpha_i - \frac{1}{2} \sum_{i,j=1}^n \alpha_i \alpha_j y_i y_j (x_i \cdot x_j) \tag{4}$$

where  $\alpha_i$  is the Lagrange multiplier corresponding to each constraint condition (2) in the original problem. This was a quadratic function optimized problem under unequal constraints; thus, there was a unique solution. It is easy to prove that only a part of (usually minority of)  $\alpha_i$  in the solution would be non-zero; the corresponding samples were support vectors, with the quantity set as  $N_s$ . When the

above problem was solved, the optimal classification function was

$$f(x) = \text{sgn}\{(w \cdot x) + b\} = \text{sgn}\left\{ \sum_{i=1}^{N_s} \alpha_i^* y_i (x_i \cdot x) + b^* \right\}, \tag{5}$$

In the above dual problem, no matter the optimization objective function (4) or classification function, (5) was only related to the inner product computation between training samples  $(x_i, x_j)$ . If the nonlinear mapping  $\Phi : \mathbf{R}^N \rightarrow \mathbf{H}$  reflected the sample of the input space to the high dimensional (may be infinite dimensional) feature space  $\mathbf{H}$ , then the training algorithm only used point product in the space when constructing the optimal hyperplane in feature space  $\mathbf{H}$ , which was  $\Phi(x_i) \cdot \Phi(x_j)$ ; and there was no individual  $\Phi(x_i)$ . Therefore, if there was a function  $K$ , then  $K(x_i, x_j) = \Phi(x_i) \cdot \Phi(x_j)$ , only the inner product computation was actually required in the higher dimensional space, which can be realized by the function in the original space, and the form of transforming  $\Phi$  was not required. According to the functional theory, provided that one kernel function  $K(x_i, x_j)$  met the Mercer condition, it corresponded to the inner product of a transformation space.

Therefore, the linear sorting after a non-linear transformation can be realized by using a proper inner product function  $K(x_i, x_j)$  as the optimal classification face; moreover, the complexity of the computation was not increased. Here the objective function (4) changes to:

$$Q(\alpha) = \sum_{i=1}^n \alpha_i - \frac{1}{2} \sum_{i,j=1}^n \alpha_i \alpha_j y_i y_j K(x_i, x_j), \tag{6}$$

The corresponding classification function also changes to

$$f(x) = \text{sgn}\left( \sum_{i=1}^{N_s} \alpha_i^* y_i K(x_i, x) + b^* \right), \tag{7}$$

This is SVM. The kernel function used in this paper was radial basis function.

$$K(x, x_i) = \exp\left(-\gamma \|x - x_i\|^2\right) \tag{8}$$

### System architecture

Figure 2 illustrates a general architecture of a BAN-based wireless BCI system. EEG sensors, along with other sensors, such as electrocardiography (ECG), electromyography (EMG), motion sensors and blood pressure sensors,

etc., send data to nearby personal server devices. Then, through a Bluetooth/WLAN connection, these data are streamed remotely to a backend system, where data analysis unit are deployed to generate the up-to-date service directives. Then, the interpreted action commands to the service response system, which performs the desired tasks according to the user's expectation. Compared to traditional BCI system, the BAN-based wireless BCI system can dramatically reduce installation complexity, wire weight, and trouble-shooting effort associated with traditional wired BCI systems. Second, the proposed BCI system would provide users with more freedom of posture and movement so that they can perform their routine tasks in real-world environments. However, the disadvantage comes from the requirements of transmitting the raw EEG data through wireless connections. In order to support the data rates, some new radio technologies, such as Ultra-Wideband (UWB), can be utilized to deal with the problem.

Compared to the architecture shown in Fig. 2, the signal processing and feature extraction are performed in the BAN (i.e., inter-BAN feature extraction). The signal processing unit is integrated into a powerful single central processor to reduce the amount of raw data, and save energy for data transmissions, as shown in Fig. 3. However, this solution also involves other challenges, such as advanced sensor data processing. It is evident that the design of system architecture should consider the performance of each design component and the specific application requirements.

## System implementation

### Experimental mode and data acquisition

In this section, we present the method for data acquisition. In the experiment, EEG signals are initiated by target and non-target stimulus in imitating a natural reading mode. The imitated natural reading mode referred to the mode that

allowed users to obtain job information from symbols without mutations, which was like reading sentences in a text under ordinary circumstances. The only difference was that in natural reading, our sight moves relative to the character sentences, whereas in imitation reading, the symbol sentences move relative to our sight, so as to avoid the EOG caused by sight movements contaminating EEG signals.

The experimental subject was code H0717, a male university student, aged 21, with normal vision, no nervous or psychological diseases, and was a paid volunteer. Four silver/silver chloride electrodes were placed according to international 10–20 electrode placement system, located at Fz, Cz, Pz, and Oz. The reference electrodes were placed at the nipples, and the forehead center was earthed. Conductive paste was smeared between electrodes and the skin to create a contact impedance less than 5 km, and the data were amplified by an HP5113 low noise amplifier; the transmission band was set as 0.1–30 Hz, and 50 Hz power frequency wave trap was set. The data acquisition system was HP4400 BOXCAR, the sampling frequency was 427 Hz.

After the above preparations, the subject sat comfortably in front of the monitor. The screen background was black, with a small window of  $16 \times 16$  pixels in the center, where the symbols in the symbol string (Fig. 4c) composed of non-target stimulus (Fig. 4b) and target stimulus (Fig. 4a) passed through the small window in the middle of screen, one by one from right to left, and at a uniform speed. The subject was required to search within this small window for the assigned target symbols contained in the symbol string (Fig. 4a) in order to induce P300.

Each record started from a short pure tone, the subject fixed his attention on the non-target smoothly moving string in the small window in order to seek out the coming target. The target stimulus would occur randomly 2–4 s after the short pure tone. Each test recording time was 1.2 s (based on the time of occurrence of target stimulus, —320 ms~880 ms), 512 samples were collected.

**Fig. 2** Architecture of a BAN-based wireless BCI system

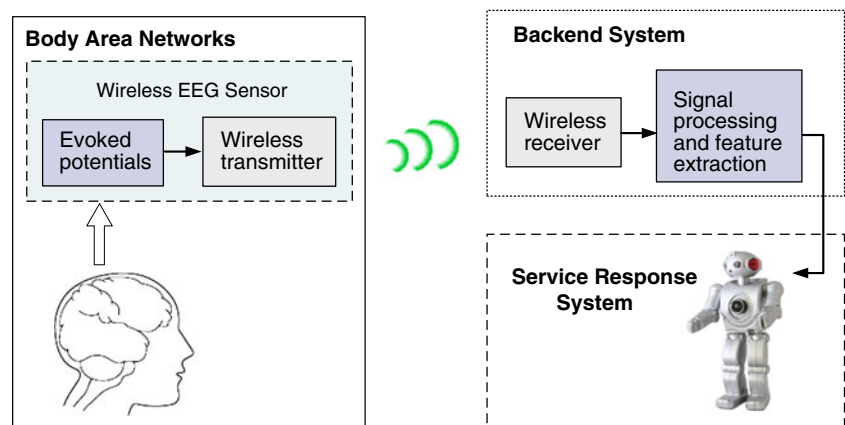
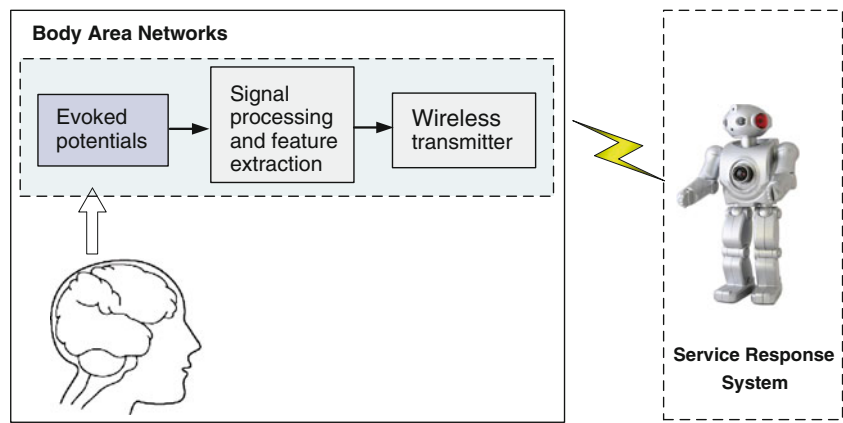


**Fig. 3** Architecture of a BAN-based wireless BCI system: inter-BAN feature extraction



Feature analysis of target stimulus evoked signal

The selection of feature parameters determined the accuracy and efficiency of the sorting algorithm. On one hand, in order to increase the recognition rate, the feature parameters should reflect the features of different modes as much as possible; on the other hand, in order to increase an efficient execution, the dimensions of the feature parameters should be as few as possible. Therefore, this study averaged the EEG signals of all selection operations of the subject synchronously, according to the channels, and made snapshots of BEAM at different times; the results are shown in Fig. 5.

According to Fig. 5, before the appearance of the target (−320 ms~0 ms), the EEG relief map of the subject was relatively smooth, and in a random low-energy state. According to the mean waveform and four head snapshots after the appearance of target, stable feature components can be induced at Fz, Cz, Pz, and Oz channels at the middle axle of the subject’s brain through testing, the peaks of N1, P2, N2, and P3 components appeared at about 100 ms, 200 ms, 250 ms, and 400 ms, respectively. This showed that the evoked potential, as resulted from the imitating natural reading evoked mode, has preferable stability. From the analysis of the waveforms of different channels, it was found that

- The amplitudes of the N1 components in the four channels were small, and almost equal to that of the EEG waveform of the non-target stimulus, if its feature separability was too low, the effect on signal classification may be too slight;

- After 200 ms latency, N2 components with large amplitude in equivalent size occurred in Fz and Cz, secondly Pz part, and there was little P2 component in Oz;
- At about 250 ms, N2 components occurred in four channels, an interesting law was that the amplitude of N2 component increased gradually from the forehead to the occiput, the latency in Oz was reduced by several ms. Therefore, it was assumed the N2 component originated from somewhere near Oz; this deduction was preliminarily proven by using the isolated component analysis method;
- P3 components can occur in four channels, the peaks occurred at about 420 ms, the amplitudes from large to small were Pz, Cz, Oz, to Fz.

Signal pre-processing

For each subject, the 512 sample data of each selection operation were recorded as MATLAB6 data files, the format was channel number × sample × job number, which was then processed as follows. First, the operation record of sample value with amplitude value greater than 45 μV was regarded as contaminated by EOG or myoelectricity and was thus discarded. Therefore, 84 target stimulus signals and 84 non-target stimulus signals were obtained from subject H, for 168 selection operation records in total. The average values were then removed from each operation record based on the mean of −200 ms~0 ms signals. Afterwards, each operation record was changed to a unit variance, which was energy normalization according to the requirements of the SVM algorithm. The above process was not related to complicated calculations, and can be quickly completed; thus, a good foundation was created for subsequent on-line real-time classifications.

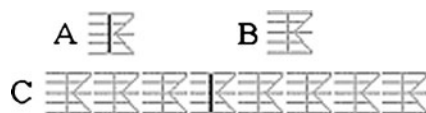


**Fig. 4** Example of induced symbol string used in this study. All the symbols were in the size of 16×16 pixels and had the same structure. **a** Target symbol, the middle separatrix was dyed red. **b** Suppressor mutation symbol (non-target stimulus), its difference to target symbol was that the middle separatrix was not dyed red. **c** The induced symbol string constructed by target symbol and suppressor mutation symbol

Single-trial estimation of target stimulus evoked signal

This study used the OSU SVM Classifier Matlab toolbox [18] as the core to construct the sorting algorithm, ν-SVM algorithm was used as the radial basis function equation, and (8) was used as the kernel function, this method was an

**Fig. 5** VEP of subject H0717 evoked by non-target stimulus (-320 ms~0 ms) and target stimulus (0 ms~880 ms), and snapshots of BEAM at different times (four black dots in middle axle of brain from top to bottom are Fz, Cz, Pz and Oz). The lateral axis is the time interval of each selection operation, the vertical axis is the mean amplitude value of EEG signals of 84 selection operations in four channels

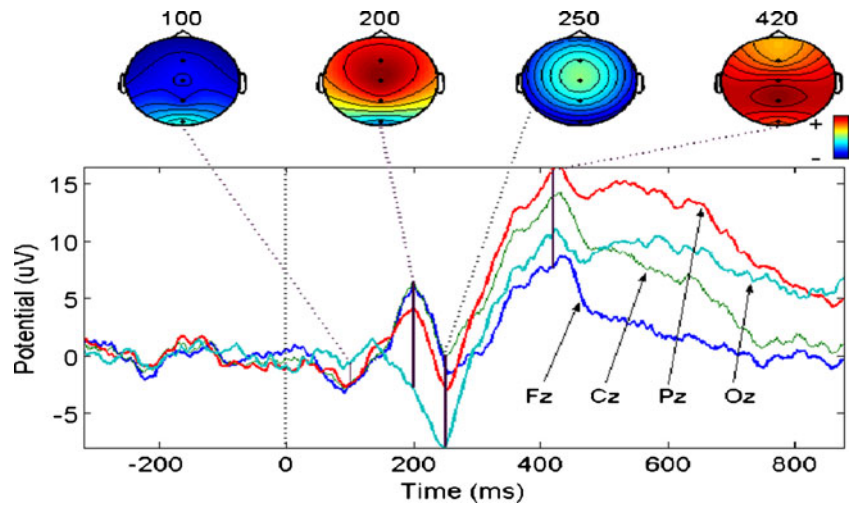


**Fig. 6** Mean average of the five forms of feature combinations

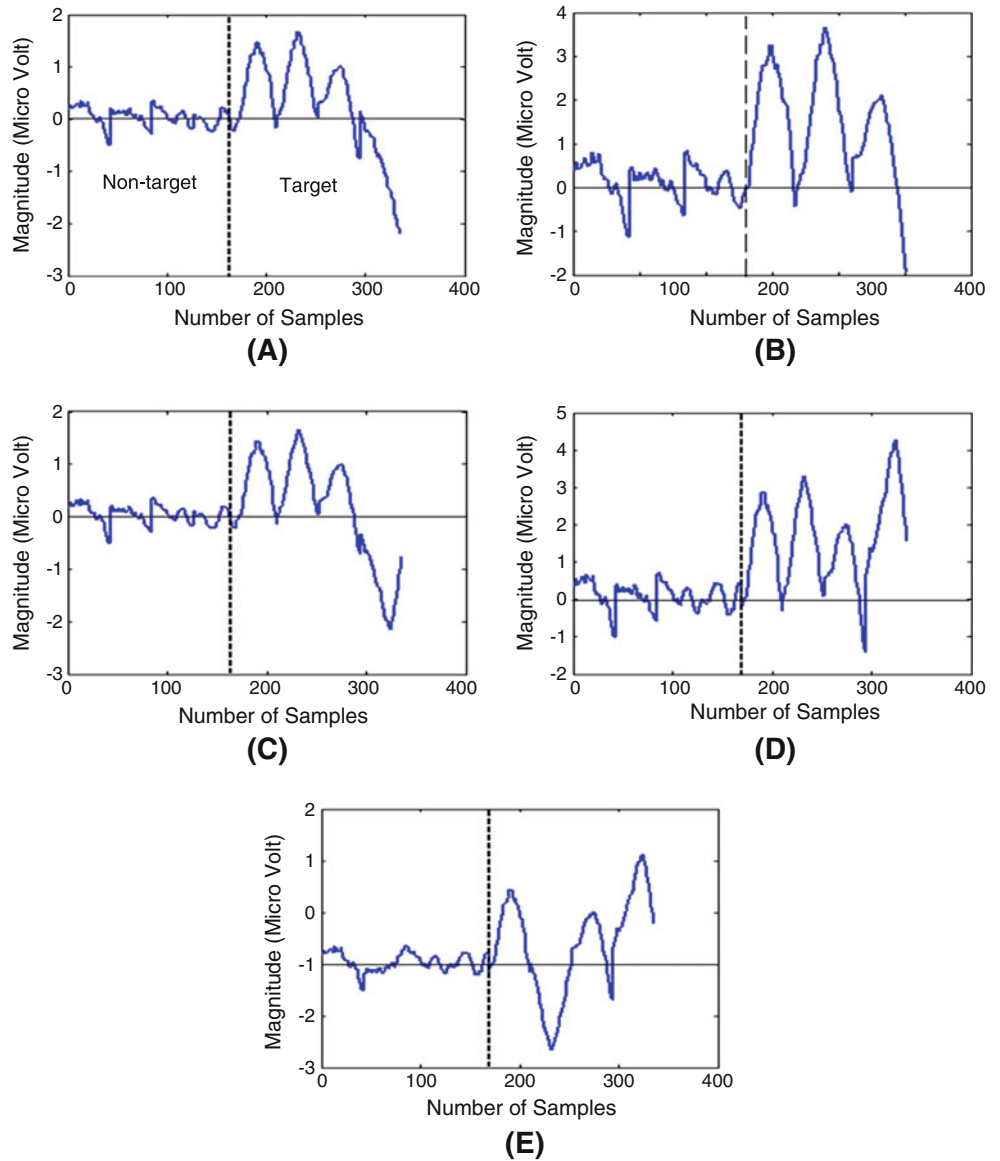


**Table 1** Experimental Results by using SVM. Each result is an average value of ten data points. (The accuracy of random selection is 50%)

Feature combination scheme	A	B	C	D	E	
SVM parameter $\gamma$	8	4	2	2	1	
$\nu$	0.3	0.3	0.3	0.7	0.64	
Accuracy(%)	Max	84.5	73.8	83	88.1	86.9
	Min	77.4	66.7	81	85.7	84.5
	Avg.	81.8	70.1	81.5	86.9	85.5

improvement on optimization problem (1), after transformation, parameter C was replaced by  $\nu$ ; thus, Eq. (1) changes to

$$\min_{w,b,\xi,\rho} \frac{1}{2} W^T W - \nu\rho + \frac{1}{l} \sum_{i=1}^l \xi_i \tag{9}$$

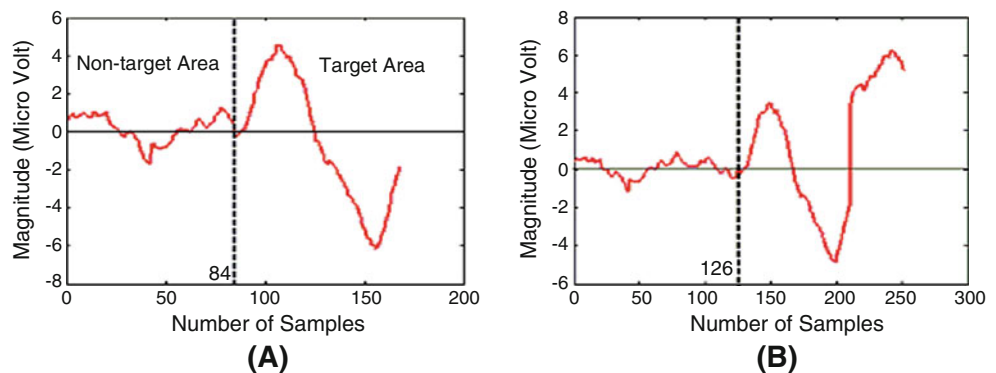
Among which,  $\nu$  is a new parameter with a range of 0~1; it is the upper boundary ratio of marginal error value to number of samples, as well as the lower boundary of ratio of support vector number to number of samples.  $\rho$  is the class interval parameter to be optimized,  $l$  is the characteristic quantity dimensions. The constraint conditions corresponding to Eq. (9) and the dual problem should also be adjusted accordingly, literature [17] could be referred for details.

In order to avoid over trained underestimation of the generalization error of the algorithm, this study divided all selection operations into two equal parts, a training data set and a test data set. Half (42) of training data set were target stimulus records, while the other half (42) were non-target stimulus records. The algorithm parameters were first optimized in the training data set, and then the test parameters were formed by using the Leave-One-Out method; finally the test data set was tested to obtain the mean recognition rate.

**Experimental results**

According to the analysis of features of target stimulus evoked signal in section Support vector machine classifier, for different feature combinations, this study used the

**Fig. 7** Mean average of the two forms of feature combinations



aforesaid method to test the subject. The experimental results are as follows.

**Test for fast feature classification**

This test used five forms of feature combinations, the idea of a feature selection was as follows: in order to apply the sorting algorithm to real-time brain-computer interface, the signals was classified as soon as possible to increase the communication speed of the overall system; short time interval signals was used for pattern feature classification when possible, and the latency of characteristic signals should be as short as possible. The combinations a and b only used 100 ms long signals within 150 ms~250 ms in several channels as the Eigen value; while combinations c, d, and e used N2 that occurred in Oz as the feature. The time interval of the overall combination was only 130 ms (150 ms~280 ms). The five feature combinations were:

- P2 components (150~250 ms) were selected from four channels for combination. The mean chart related to feature combination was as shown in Fig. 6a.
- P2 components (150~250 ms) were selected from channels 1, 2 to 3 for combination as seen in Fig. 6b.
- P2 components (150~250 ms) were selected from channels 1, 2 to 3, and N2 component (180~280 ms) was selected from channel 4, as shown in Fig. 6c.
- P2 components (150~250 ms) were selected from channels 1, 2 to 3, and N2 component (180~280 ms) was selected from channel 4; but N2 component had phase inversion (N2=--N2), as seen in Fig. 6d.
- Same as above, but channel 2 had phase inversion, as shown in Fig. 6e.

The analysis results of features of target stimulus and non-target stimulus are shown in Table 1.

**Test with small number of channels and feature dimensions**

This test used two forms of feature combinations, the idea of feature selection was as follows: the number of channels

**Table 2** For combination A in Fig. 7, experimental results by using SVM and its corresponding best parameters. Each result is an average value of ten data points. (The accuracy of random selection is 50%).

Sample frequency		427 Hz	213 Hz	107 Hz	53 Hz
SVM parameter	$\gamma$	5	5	5	5
	$\nu$	0.01~0.4	0.01~0.4	0.01~0.4	0.01~0.4
Accuracy(%)	Max	94	86.9	86.9	82.1
	Min	91.7	85.7	82.1	78.6
	Avg.	92.1	86.1	85.1	80.2

and feature dimensions was as few as possible; the signal time interval was as short as possible; short time interval signal contents with the most obvious feature in four channels were selected. According to Fig. 5, P2 was the most obvious in channel Fz, N2 was the most obvious in channel Oz, and P3 had the maximum amplitude value in all channels.

Combination A: Figure 7a shows the combination of P2 (150 ms~250 ms) in channel Fz and N2 (180 ms~280 ms) in channel Oz. For such combination, the result of feature classification is as shown in Table 2.

Combination B: Figure 7b shows the combination of P2 (150 ms~250 ms) in channel Fz and N2 (180 ms~280 ms) and P3 (350 ms~450 ms) in channel Oz; for such combination, the result of feature classification is as shown in Table 3.

## Discussions

According to the above tests, the selection of characteristic quantity was very important for improving classification accuracy.

1. Using only the P2 component as the characteristic quantity cannot attain satisfactory classification effects (see combination b in Table 1, recognition rate was only 70%).

**Table 3** For combination B in Fig. 5, experimental Results by using SVM and its corresponding best parameters. Each result is an average value of ten data points. (The accuracy of random selection is 50%).

Sample Frequency		427 Hz	213 Hz	107 Hz	53 Hz
SVM parameter	$\gamma$	2~4	2~4	2~4	2~4
	$\nu$	0.01~0.5	0.01~0.5	0.01~0.5	0.01~0.5
Accuracy(%)	Max	100	100	98.8	97.6
	Min	98.8	98.8	98.8	94
	Avg.	98.8	98.8	98.8	96.4

In order to reduce feature dimensions, the data is sampled and the classified results are compared

2. The classification accuracy can be increased through the phase inversion of N2 component in the combination feature (in comparison to columns c and d in Table 1), whereas P2 phase inversion would not result in this phenomenon (in comparison to columns d and e in Table 1).
3. Higher dimensions of characteristic quantity did not mean higher classification accuracy (compare Table 1 and Table 2); therefore, the significance level of characteristic quantity and the stability of each selection operation were decisive. According to the comparison between the classification accuracy of 92.1% in Table 2 and the combination c (classification accuracy of 81.5%) in Table 1, the former used two less channels' P2 features than the latter, and the classification accuracy was increased by 10%. In order to decipher this puzzle, the EEG relief map of multiple selection operations of four channels was analyzed; and it was found that the amplitude of P2 component in channel Fz was larger than that in other channels at 200 ms after target stimulus, and it appeared steadily in most tests. Whereas, P2 became increasingly weak in Cz and Pz, and the number of absent was increased at 200 ms. Such instability of components occurred directly in the feature space; thus, the distribution of similar patterns became increasingly messy, and non-linearity was increased. Hence, the classification accuracy declined.
4. In order to accelerate classification and reduce the amount of calculations, the feature dimensions was as low as possible. According to the results in Tables 2 and 3, P2

In order to reduce feature dimensions, the data is sampled and the classified results are compared



and N2 features were sensitive to sampling frequency, when P3 features with larger weights were added, the sampling frequency was reduced by 75%; the classification accuracy was almost uninfluenced. It showed that the frequency involved in the signal features of P2 and N2 components was high; whereas, the P3 component had only a low frequency component.

5. According to Table 2, the classification accuracy of 92% can be attained only by using 100 ms data of two channels as the characteristic quantity, which was very important for increasing the overall communication speed of brain-controlled spelling devices. The analysis shows that the speed of the brain-controlled spelling device, constructed using the evoked EEG signals generated by the imitating human natural reading evoked mode as carriers, would be 5~20 times of that of the existing devices, or above 90 bit/min [19].
6. Table 3 shows that an almost perfect pattern classification effect can be reached using the optimal feature combination of P2, N2, and P3. As this combination was not overly sensitive to sampling frequency, it can greatly reduce the feature dimensions and increase the classification speed.

## Conclusions

To use the new man-machine interactive mode, brain-computer interface to construct brain-controlled spelling devices, single recognition of communication carrier signals must be realized. SVM is a non-linear classifier, as its optimization procedure is completed only by its support vectors. Moreover, it is fast and has good generalization ability, and is especially applicable to the classification of EEG signals with some non-linear behaviors. This algorithm is very sensitive to parameters  $\nu$  and  $\gamma$ ; thus, it must be carefully determined. Since the selection of characteristic quantity is very important for classification accuracy, this paper combined the feature components from four tested channels for research. The results show that higher dimensions of characteristic quantities, or more feature components, did not translate into higher classification accuracy. The classification accuracy rate of 92% can be obtained only by using the short 100 ms data of P2 from Fz and N2 from Oz as the feature for pattern classification. When the characteristic quantity P3 component was added, the feature dimensions can be greatly reduced by down sampling for frequency division, and the mean classification accuracy rate was 98.8%, the perfection of 100% can be reached. These results create a good foundation for

increasing the overall communication speed of the brain-computer interface.

## References

1. Ullah, S., Higgins, H., Braem, B., Latre, B., Blondia, C., Moerman, I., et al., A comprehensive survey of wireless body area networks: On PHY, MAC, and network layers solutions. *J. Med. Syst.*, 2010. doi:10.1007/s10916-010-9571-3.
2. El-Nasr, M., and Vasilakos, A., DigitalBeing-using the environment as an expressive medium for dance. *Inf. Sci.* 178(3):663–678, 2008.
3. Lotte, F., et al., A review of classification algorithms for EEG-based brain-computer interfaces. *J. Neural Eng.* 4(1):1–13, 2007.
4. Bashashati, A., et al., A survey of signal processing algorithms in brain-computer interfaces based on electrical brain signals. *J. Neural Eng.* 4(1):32–57, 2007.
5. Cinar, E., and Sahin, F., A study of recent classification algorithms and a novel approach for EEG data classification. *IEEE Int. Conf. Syst. Man and Cybernetics (SMC)*, 3366–3372, 2010
6. Kamel, N., Yusoff, M., and Mohammad, H., Single-trial subspace-based approach for VEP extraction. *IEEE Trans. Biomed. Eng.*, PP(99):1, 2011
7. Kaper, M., Meinicke, P., Großekathöfer, U., Lingner, T., and Ritter, H., BCI competition 2003—data set IIb: Support vector machines for the P300 speller paradigm. *IEEE Trans. Biomed. Eng.* 51:1073–1076, 2004.
8. Salvaris, M., and Sepulveda, F., Visual modifications on the P300 speller BCI paradigm. *J. Neural Eng.* 6(2):1–8, 2009.
9. Hoffmann, U., et al., An efficient P300-based brain-computer interface for disabled subjects. *J. Neurosci. Meth.* 167(1):115–125, 2008.
10. Wolpaw, J. R., et al., Brain-computer interface technology: A review of the first international meeting. *IEEE Trans. Rehab. Eng.* 8:166–173, 2000.
11. Xie, Q. L., Yang, Z. L., Chen, Y. G., and He, J. P., BCI based on imitating-reading-event-related potentials [A]. In *Proc. Of 7th world multiconference on systemics, cybernetics and informatics*, XIII:49–54, 2003
12. Chen, M., Gonzalez, S., Vasilakos, A., Cao, H., and Leung, V., “Body area networks: A survey”, *ACM/springer mobile networks and applications (MONET)*, 16(2):171–193, April 2010
13. Pedrycz, W., and Vasilakos, A. V., Linguistic models and linguistic modeling. *IEEE Trans. Syst. Man Cybernet. B* 29(6):745–757, 1999.
14. Ullah, S., Khan, P., Ullah, N., and Kwak, K., MAC-bridging for Multi-PHYs communication in BAN. *Sensors* 10(11):9919–9934, 2010.
15. Ullah, S., and Kwak, K., An ultra low-power and traffic-adaptive medium access control protocol for wireless body area network. *J. Med. Syst.*, 2010. doi:10.1007/s10916-010-9564-2.
16. Lin, C., Ko, L., Chang, M., et al., Review of wireless and wearable electroencephalogram systems and brain-computer interfaces—a mini-review. *Gerontology* 56:112–119, 2010.
17. Chang, C.-C., and Lin, C.-J., Training support vector classifiers: Theory and algorithms. *Neural Comput.* 13:2119–2147, 2001.
18. Ma, J., Zhao, Y., and Ahalt, S., OSU SVM classifier matlab toolbox [Online] [http://www.support-vector-machines.org/SVM\\_soft.html](http://www.support-vector-machines.org/SVM_soft.html), 2002
19. Guan, J., Chen, Y., Lin, J., Designing a dual page virtual keyboard for mental speller[A]. In *proc. of the first int. conf. on neural interface and control*, Wuhan, May, 2005